

# Dynamical topology and statistical properties of spatiotemporal chaos

Quntao Zhuang<sup>1</sup>, Xun Gao<sup>1</sup>, Qi Ouyang<sup>1,2,3</sup>, and Hongli Wang<sup>1,2\*</sup>

<sup>1</sup>State key Laboratory for Mesoscopic Physics and School of Physics, Peking University, Beijing 100871; <sup>2</sup>Center for Quantitative Biology, Peking University, Beijing 100871; <sup>3</sup>The Peking-Tsinghua Center for Life Sciences at School of Physics, Beijing 100871, China

For spatiotemporal chaos described by partial differential equations, there are generally locations where the dynamical variable achieves its local extremum or where the time partial derivative of the variable vanishes instantaneously. To a large extent, the location and movement of these topologically special points determine the qualitative structure of the disordered states. We analyze numerically statistical properties of the topologically special points in one-dimensional spatiotemporal chaos. The probability distribution functions for the number of point, the lifespan, and the distance covered during their lifetime are obtained from numerical simulations. Mathematically, we establish a probabilistic model to describe the dynamics of these topologically special points. In despite of the different definitions in different spatiotemporal chaos, the dynamics of these special points can be described in a uniform approach.

**Spatiotemporal chaos is often mediated by certain types of dynamical spatial structures or topological features such as defects in defect-mediated turbulence. The dynamics of such special entities characterizes the disordered states and presents a simplified description of spatiotemporal chaos. For the more general spatiotemporal chaos that are not featured by defects and apparent geometrical structures, it is a challenge to obtain a quantitative mathematical characterization that records or preserves qualitatively the geometric structures of the complex patterns. In this paper, we propose to use the topologically special points such as extremum and critical points in disordered states to characterize qualitative properties of spatiotemporal chaos. To a large extent, the location and movement of these topologically special points determine the qualitative structure of the disordered states. We calculate statistical properties of the extremum and critical points with the Brusselator model and the complex Ginzburg-Landau equation. A probabilistic model that can regenerate the simulation results is proposed.**

Spatially extended dynamical systems may exhibit spatiotemporal chaos (STC) characterized by a finite correlation length in both space and time [1]. While self-organization in pattern formation systems has been intensively investigated in the last decades, high-dimensional disordered states are still poorly understood. The main challenge in this field has been to reveal the onset of STC [2–4] and to establish methods to characterize such disordered states [1, 5, 6]. In many spatially extended systems, spatiotemporal chaos is characterized by the presence of defects. For such disordered states generally referred to as defect-mediated turbulence (DMT), a statistical description of defect dynamics has been used as a unifying approach to characterize such STCs [7–17]. Numerical and theoretical analyses have been carried out in the complex Ginzburg-Landau equation [7, 8], the FitzHugh-Nagumo-type system [9], the Willamowski-Rössler model [10], the model for rotating non-Boussinesq convection [11], and catalytic surface reactions [12]. Experimental studies of defect statistics have been also reported from electro-convection in liquid crystals [13, 14], the catalytic surface reaction [15], and the Belousov-Zhabotinsky reaction [16].

Similar to the defects in DMTs, other spatial structures or topological features have been used to quantify the dynamical complex patterns. Such examples have been reported from algebraic topology for measuring the complexities in disordered states [18], instantaneous stagnation points with vanishing velocity in the velocity field of fluids [19], and self-replicating spots in the Gray-Scott model [20, 21].

In order to understand and quantify the more general STCs that are not featured by defects and apparent geometrical structures, we here propose a quantitative mathematical characterization that records or preserves the dynamical structures of disordered states. For STCs described by partial differential equations, there are generally locations  $r_0$  in the scalar field  $X(r, t)$  where the dynamical quantity achieves its local extremum, *i.e.*,

---

\*To whom correspondence should be addressed, E-mail: hlwang@pku.edu.cn

$\frac{\partial X(r,t)}{\partial r}|_{r_0} = 0$ , as depicted in Fig. 1a. These instantaneous maximum or minimum points preserve the geometrical structures of the disordered states (Fig. 1c). If the locations and movements of all of these special points are known, the pattern can be primarily determined. Similarly, as in the velocity field of fluid flows [19], the spatiotemporal chaotic field  $X(r,t)$  can be characterized by locations  $r_0$  where the time partial derivative of the dynamical quantity vanishes instantaneously, *i.e.*,  $\frac{\partial X(r,t)}{\partial t}|_{r_0} = 0$ , as demonstrated in Fig. 1b. These critical points carry the bulk of the information contained in the disordered patterns (Fig. 1d). Such defined topologically special points, which are present even in ordered states, are distinct from the topological defects in previously studied DMTs. They are created and annihilated irregularly in pairs, changing simultaneously the topological structures of the disordered states. To a large extent, the location and movement of these points determine the qualitative structure of the disordered states.

We analyze numerically statistical properties of the topologically special points in one-dimensional STCs with the Brusselator model and the complex Ginzburg-Landau equation (CGLE). The probability distribution functions (PDF) for the number of extremum points and that of critical points are obtained from numerical simulations. PDFs for the lifespan as well as the distance covered during the lifetime are also calculated. Mathematically, we establish a probabilistic model to describe the dynamics of these topologically special points. The analysis gives results that are in good agreement with numerical simulations. In despite of the different definitions in different STCs, the dynamics of these special points can be described uniformly.

*Models and numerical results.*— The reaction-diffusion system with Brusselator reaction kinetics is a standard model system for the investigation of self-organized structures in nonlinear chemical reactions, which is governed by the following set of partial differential equations [22],

$$\partial_t X = D_X \partial_r^2 X + X^2 Y - (B + 1)X + A, \quad (1)$$

$$\partial_t Y = D_Y \partial_r^2 Y - X^2 Y + BX. \quad (2)$$

Figure 1 demonstrates the chemical turbulence generated by Eqs. 1 and 2 with parameters  $A = 2.0, B = 5.5, D_X = 1, D_Y = 0$ . Figure 1a and 1b depict the snapshots of the one-dimensional fields  $X(r,t)$  and  $\frac{\partial X(r,t)}{\partial t}$ , respectively. The maximum (minimum) points in Fig. 1a are denoted as red (blue). The dots in Fig. 1b are for the critical points where  $\frac{\partial X(r,t)}{\partial t} = 0$ , with the red or blue for locations where  $\partial_r[\partial_t X(r,t)] > 0$  or  $\partial_r[\partial_t X(r,t)] < 0$ . As these special points demonstrated in Fig. 1a and 1b are always created and annihilated in red-blue pairs, the red and the blue can be denoted with positive (+) and negative (-) signs similar to the positive and negative charges for topological defects in DMTs. The space-time plots in Fig. 1c and 1d demonstrate the time evolutions of

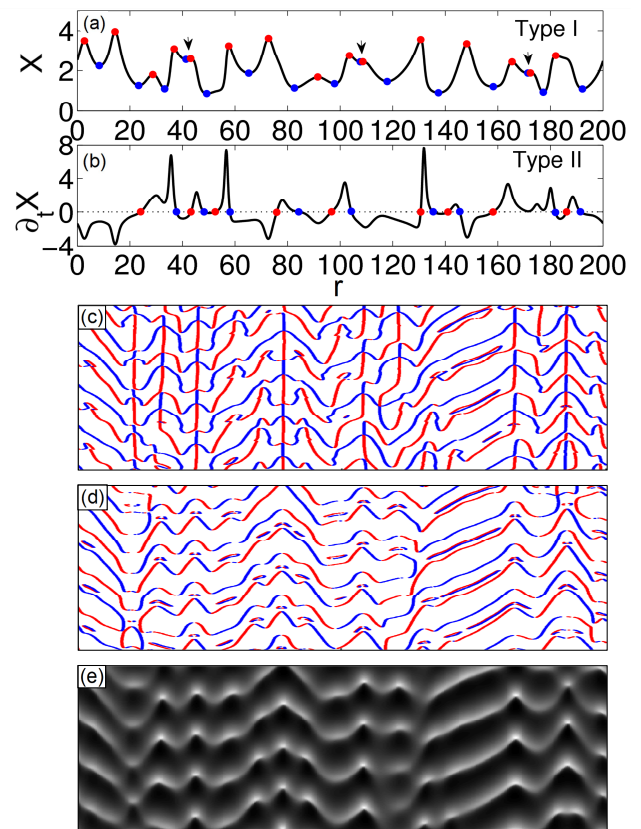


FIG. 1: One-dimensional spatiotemporal chaos generated from the reaction-diffusion system with Brusselator reaction kinetics (Eqs. 1 and 2). (a) Snapshot of  $X(r,t)$  and local maximum (red) and local minimum (blue) points; (b) Snapshot of  $\partial_t X(r,t)$  and critical points where  $\partial_t X(r,t) = 0$ , with red for  $\partial_r[\partial_t X(r,t)] > 0$  and blue for  $\partial_r[\partial_t X(r,t)] < 0$ . (c) and (d) are space-time plots (horizontal space and vertical time) depicting the time evolutions of the topological special points in (a) and (b), respectively. (e) The space-time map of  $X(r,t)$  coded in gray scales. The arrows in (a) indicate the red-blue pairs being created or annihilated in the disordered states. Parameters:  $A = 2.0, B = 5.5, D_X = 1, D_Y = 0$ . Periodic boundary conditions are used in simulations.

the topologically special points in Fig. 1a and Fig. 1b, respectively. The gray-scaled space-time pattern in Fig. 1e is generated from  $X(r,t)$ . To a large extent, the complexities of the disordered states (Fig. 1e) are primarily preserved or recorded in the time evolutions of these topological points (Fig. 1c and 1d). The definitions of the special points for the Brusselator can be easily extended to the CGLE and other systems. The CGLE which is one of the most-studied nonlinear equations in physics is given by [23],

$$\partial_t A = A + (1 + ic_1)\partial_r^2 A - (1 - ic_3)|A|^2 A. \quad (3)$$

Beyond the Benjamin-Feir instability, three types of chaotic behavior are possible in the one-dimensional CGLE, namely phase turbulence, space-time defect turbulence [24], and intermittency [25]. As the emphasis of

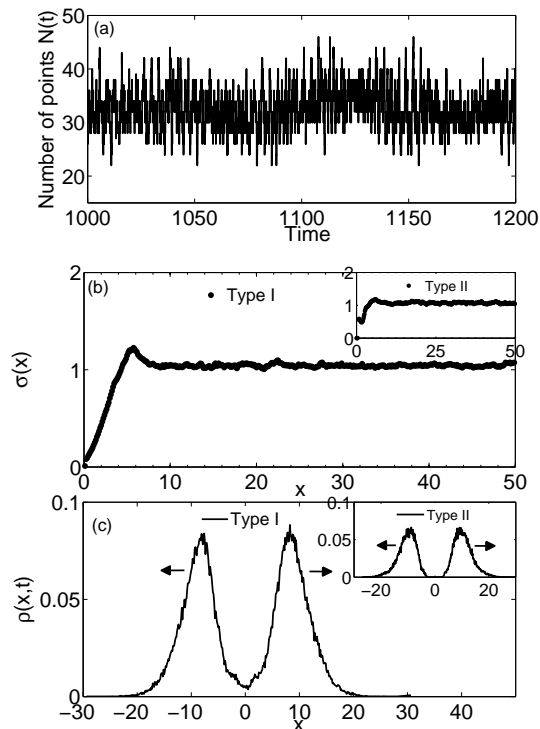


FIG. 2: (a) Time series  $N(t)$  for the number of extremum points. (b) The normalized pair correlation function  $\sigma(r)$  for the extremum points (inset for the critical points). (c) Bimodal probability density function  $\rho(x, t = 2.5)$  for extremum points (inset for critical points). The arrows indicate the directions  $\rho(x, t)$  is splitting. All the simulation results are obtained from the Brusselator model with the same parameters in Fig. 1.

this paper is on the presentation of the technique, we here concentrate on the topological special points as defined for the Brusselator without discrimination in the types of STCs.

As a simplified representation of spatiotemporal chaos, the dynamical behavior of extremum and critical points are more convenient to describe and cope with. The points perform diffusive and drift motions in the space after they are created in pair, are destroyed when two neighboring points with opposite sign bump into each other. The processes occur continuously and indefinitely, and the spatiotemporal pattern looks like a chaotic “soup”. The number of extremum or critical points in the disordered pattern undergoes fast fluctuations. Figure 2a illustrates a time series  $N(t)$  of the number of extremum point calculated from the Brusselator. The fast stochastic fluctuations in  $N(t)$  is a manifestation of the disorder and incoherence in the turbulence. Figure 2b demonstrates the pair correlation functions for the extremum and critical points, showing short range interactions between these points.

The diffusive and drift motion of extremum and critical points can be examined from the time dependent prob-

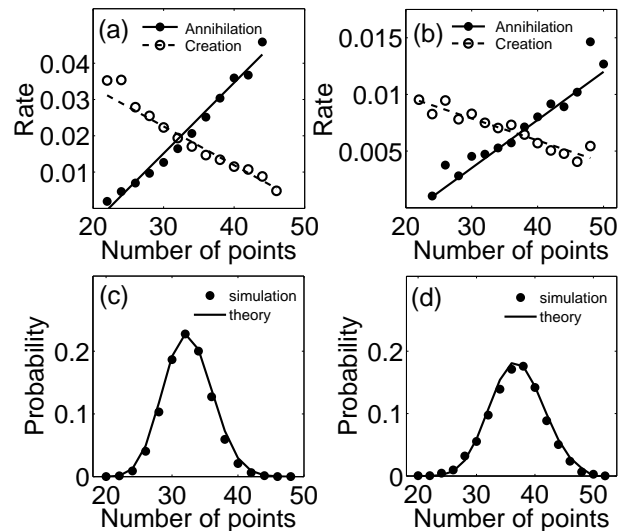


FIG. 3: Numerically simulated gain and loss rates, which are approximately linear functions, for extremum points obtained from the Brusselator model (a) and critical points from the CGLE (b), and probability distribution functions for the number of extremum points obtained from the Brusselator (c) and of critical points from the CGLE. Theoretical PDFs from Eq. 4 are depicted as solid lines.

ability density function  $\rho(x, t)$  for the distance  $x$  that a point travels from the location where it is created at the time  $t$  from the moment it is created. This can be calculated by tracking the points from their creation to annihilation processes. Apparently the initial distribution  $\rho(x, 0)$  is a delta function  $\delta(x)$ . As demonstrated in Fig. 2c, it will then split as the pairs of point that are newly born with opposite signs move apart, forming a bimodal distribution  $\rho(x, t)$ . By monitoring the creation and annihilation events, the gain and loss rates can be obtained numerically (Fig. 3a and 3b). Both are approximately linear functions in the number of points in the system. From the time series  $N(t)$ , the probability density function (PDF)  $P(N)$  which is the probability for finding  $N$  points in the disordered states can be derived. Figure 3c and 3d (dots) demonstrate the PDFs for the extremum and critical points obtained from the Brusselator and the CGLE, respectively.

By monitoring the creation, movement, and annihilation processes of these points, we derive two extra properties: the probability density function  $P(\tau)$  for the life span  $\tau$  of the special points, and the distribution  $P(\lambda)$  of the displacement  $\lambda$  (i.e., the distance a point covers during its lifetime). Figure 4 (dots) demonstrates the life span distributions for extremum and critical points calculated separately from the Brusselator model (Fig. 4a) and the CGLE (Fig. 4b). They are uniformly exponential decays. Figure 5 (dots) depicts the distribution of displacement  $\lambda$  for extremum and critical points in the Brusselator model (Fig. 5a) and CGLE (Fig. 5b),

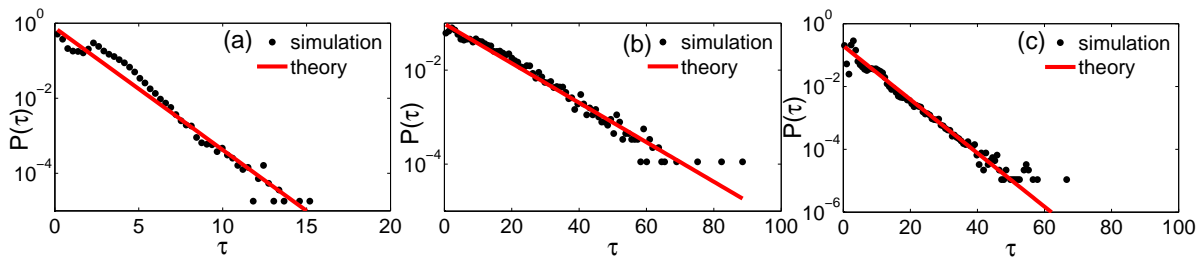


FIG. 4: Lifetime distribution  $P(\tau)$  of the topologically special points obtained from numerical simulations (black dots) and from theoretical prediction of Eq. 9 (red line). (a) Extremum points in the Brusselator model,  $C = 0.7482$ ; (b) Critical points in the CGLE,  $C = 0.1964$ . (c) Critical points in the autocatalator model,  $C = 0.09669$ .

respectively. The distributions are also uniformly tent-shaped. The left-right symmetry in the distributions is due to the symmetrical splitting movement of the special points after they are created.

*Theoretical analysis.*— We now seek to establish a probabilistic model to generate quantitatively the numerical results. The topologically special points we defined here are similar to defects in DMTs. The master equation description of defect dynamics [7] can be extended in straightforward to the situation we consider here. The probability distribution function for the number of extremum or critical point can be readily expressed as [7],

$$P(N) = P(0) \prod_{j=0}^{N-1} \frac{\Sigma_+(j)}{\Sigma_-(j+1)}, \quad (4)$$

where  $\Sigma_+$  and  $\Sigma_-$  are, respectively, gain and loss rates that define the transition rates of the Markov chain. From our simulations,  $\Sigma_+$  and  $\Sigma_-$  for the Brusselator and the CGLE are well approximated by linear dependence on  $N$ ,  $\Sigma_+(N) = c_0 + c_1 N$ ,  $\Sigma_-(N) = a_0 + a_1 N$  (solid lines in Fig. 3a and 3b). The resulting distributions from Eq. 4 are depicted in Fig. 3c and 3d (curves) which are in good agreement with simulations in despite that the special points are different and in different models.

Our finding that the creation and annihilation rate of the special points are both linear with  $N$  is distinct from previous findings in 2D DMT where the annihilation rate is proportional to  $N^2$  [7]. The difference might be due to that different dimensions have been considered. The  $N^2$  annihilation rate is intuitive in 2D systems. In 1D systems as we consider, the positive spots and negative spots are alternatively distributed in the 1D space. As an elementary annihilation or creation event occurs between two spots with opposite signs, it is correlated with two neighboring spots. The annihilation/creation rates should thus be proportional to the number of spot pairs in the space and would result in the linear dependence on  $N$  as we observed.

In order to analyze the behaviors of topologically special point in more detail, an equation for the probability density function  $\rho(x, t)$  needs to be established. As observed in our simulations, the extremum and critical

points perform drifting and diffusive motion (Fig. 2c), and suffer random extinctions during these processes. To describe these properties, we propose a modified Fokker-Planck equation for the time evolution of  $\rho_+(x, t)$  and  $\rho_-(x, t)$  with  $\rho(x, t) = (\rho_+(x, t) + \rho_-(x, t))/2$ ,

$$\partial_t \rho_{\pm}(x, t) = \{\mp v \partial_x + D \partial_x^2 - [c \sum_i \delta(x - x_i(t))]\} \rho_{\pm}(x, t). \quad (5)$$

The sign  $\pm$  describes the symmetrical splitting of  $\rho(x, t)$  into  $\rho_+$  and  $\rho_-$ . In Eq. 5, constant drifting and diffusion are assumed. The right most term is used to model interaction decays, where  $x_i(t)$  is the location of a special point leading to the decay. In a mean-field approximation, the last term is proportional to the normalized pair correlation function  $\sigma(x)$  (Fig. 2b). One has  $\langle c \sum_i \delta(x - x_i(t)) \rangle_t = c \sigma(x)$ . Due to that  $\sigma(x)$  approaches a constant value beyond a small spatial correlation in STC, one has,

$$\frac{\partial}{\partial t} \rho_{\pm}(x, t) = \{\mp v \frac{\partial}{\partial x} + D \frac{\partial^2}{\partial x^2} - C\} \rho_{\pm}(x, t). \quad (6)$$

The above equation has the solution

$$\rho_{\pm}(x, t) = \frac{1}{\sqrt{4\pi Dt}} \exp[-\frac{(x \mp vt)^2}{4Dt}] \exp(-Ct). \quad (7)$$

The probability  $\rho(x, t)$  is thus,

$$\rho(x, t) = (\rho_+(x, t) + \rho_-(x, t))/2. \quad (8)$$

The life span distribution  $P(\tau)$  can be calculated directly from the decreasing of the total probability,

$$P(\tau) = -\frac{d}{d\tau} \int_{-\infty}^{\infty} \rho(x, \tau) dx = C \exp(-C\tau). \quad (9)$$

The probability is exactly an exponentially decaying function where  $C$  depends on the detailed short-range interactions. This theoretical result is in good agreement with numerical results as shown in Fig. 4a and 4b.

To calculate the distribution of displacement  $P(\lambda)$ , we have the probability density for the annihilation at location  $x$  with life time  $\tau$  as  $\rho_F(x, \tau)P(\tau)$ , where  $\rho_F(x, t) =$

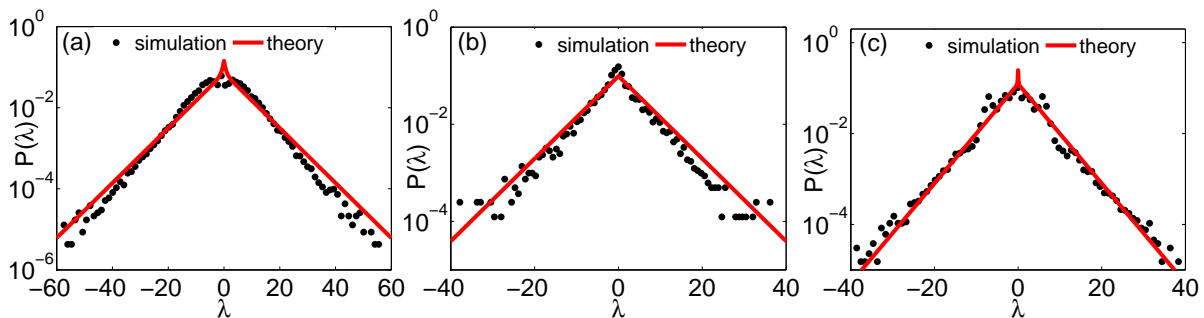


FIG. 5: Displacement distribution  $P(\lambda)$  for the special points obtained from numerical simulations (black dots) and from theoretical predictions of Eq. 11 (red line). (a) for extremum points in the Brusselator model,  $v = 4.331$ ,  $D = 2.9925$ ; (b) for critical points in the CGLE,  $v = 0.764$ ,  $D = 0.0601$ ; (c) for critical points in the autocatalator model,  $v = 3.0$ ,  $D = 2.526$ . The values of  $C$  are as in Fig. 4.

$(\rho_+(x, t) + \rho_-(x, t))/2|_{C=0}$  is the solution of Eq. 6 with  $C = 0$ . The free path length distribution  $P(\lambda)$  is,

$$P(\lambda) = \int_0^\infty d\tau \rho_F(\lambda, \tau) P(\tau). \quad (10)$$

The integration leads to,

$$P(\lambda) = \frac{C}{\sqrt{4CD+v^2}} \exp\left[-\frac{\lambda}{2D}(\sqrt{4CD+v^2})\frac{\lambda}{|\lambda|}\right] \times (\exp[-v\lambda/2D] + \exp[v\lambda/2D])/2. \quad (11)$$

For a specific disordered state, the drift velocity  $v$  and diffusion coefficient  $D$  in the above equation can be determined from the simulations of  $\rho(x, t)$  (refer to Fig. 2c) using Eq. 8, and the constant  $C$  can be determined from the simulated life span distribution according to Eq. 9. With these parameters, the theoretical result predicted by Eq. 11 for the extremum and critical points the Brusselator and in the CGLE demonstrated in Fig. 5a and 5b (curves), respectively, which also agree uniformly well with the results obtained from direct simulations.

*Summary and Conclusion.*— In summary, we have proposed using topologically special points such as extremum and critical points in disordered states to characterize the qualitative properties of spatiotemporal chaos that is not mediated by defects. The special points can be denoted as positive or negative, and undergo pairwise interactions, changing the topological structures of the disordered states when they are created and annihilated. The dynamics of such points are similar to the  $A+B \rightleftharpoons C$  type chemical reaction in 1D space [26], where different reactants  $A$  and  $B$  combine into resultant  $C$  when they encounter and  $C$  decomposes into  $A$  and  $B$ . We have checked the dependence of the average on the length of the system (data not presented here). The average number of special points is proportional to the size of the system and is therefore extensive in spatiotemporal chaos.

We demonstrated with the Brusselator model and the CGLE that the dynamics of special points determining the qualitative properties of STCs can be described in a probabilistic model, in spite of different definitions of the

special points and different dynamical systems. Specifically, the previous statistical description of defect dynamics in defect-mediated turbulence was extended to the general spatiotemporal chaos. A modified Fokker-Planck equation was proposed as a uniform description for the drifting, diffusive and extinctions processes. Theoretical analysis gives explicitly expressions for the lifespan distribution and the displacement distribution, and predicts correctly numerical simulation results.

The definition of the topological and dynamical special points and the probabilistic approach that we proposed for 1D STCs in the Brusselator and CGLE can be extended to other disordered states. For instance, we have analyzed the chemical turbulence which emerges from the instability of a traveling wave. The model is a two-variable, cubic autocatalator with equal diffusivities of the species which is described by the following equations [27],

$$\partial_t \alpha = \delta \partial_z^2 \alpha + 1 - \alpha - \mu \alpha \beta^2, \quad (12)$$

$$\partial_t \beta = \partial_z^2 \beta + \mu \alpha \beta^2 - \phi \beta. \quad (13)$$

As demonstrated in Fig. 4c, the lifetime distribution of the critical points obtained from numerical simulations (black dots) in the STC regime, with  $\delta = 1$ ,  $\phi = 3.0$ ,  $\mu = 38.0$ , is in satisfactory agreement with that predicted by Eq. 9 (red line). Figure 5c depicts the same agreement between the numerical simulation and theoretical prediction of the displacement distribution.

In 2D defect-mediated turbulence, the defect is a convenient characterization of turbulence as previously investigated. The method present here is suitable only for 1D systems. It is convenient to define and handle topologically special points in 1D systems. In 2D systems, the special points as we defined in 1D would be no longer isolated points, but could be connected into 1D lines or filaments.

The work is financially supported by the NSFC (10721403, 11074009, 10774008, 11174013) and MSTC (2009CB918500).

- 
- [1] M. C. Cross and P. C. Hohenberg, *Rev. Mod. Phys.* **65**, 851 (1993).
- [2] D. Ruelle and F. Takens, *Commun. Math. Phys.* **20**, 167 (1971).
- [3] Z. Qu, J. N. Weiss, and A. Garfinkel, *Phys. Rev. Lett.* **78**, 1387 (1997).
- [4] F. Brochard, E. Gravier, and G. Bonhomme, *Phys. Rev. E* **73**, 036403 (2006).
- [5] P. Manneville, in *Macroscopic Modelling of Turbulent Flows*, Springer, Berlin, 1985.
- [6] D. A. Egolf and H. S. Greenside, *Nature*, **369**, 129 (1994); *ibid*, *Phys. Rev. Lett.* **74**, 1751 (1995).
- [7] L. Gil, J. Lega, and J.L. Meunier, *Phys. Rev. A* **41**, 1138 (1990).
- [8] H. Wang, *Phys. Rev. Lett.* **93**, 154101 (2004);
- [9] M. Hildebrand, M. Bär, and M. Eiswirth, *Phys. Rev. Lett.* **75**, 1503 (1995).
- [10] J. Davidsen and R. Kapral, *Phys. Rev. Lett.* **91**, 058303 (2003);
- [11] Y. N. Young and H. Reicke, *Phys. Rev. Lett.* **90**, 134502 (2003).
- [12] D. Krefting and C. Beta, *Phys. Rev. E* **81**, 036209 (2010).
- [13] K. E. Daniels and E. Bodenschatz, *Phys. Rev. Lett.* **88**, 034501 (2002).
- [14] K. E. Daniels and E. Bodenschatz, *Chaos* **13**, 55 (2003).
- [15] C. Beta, A. S. Mikhailov, H. H. Rotermund, and G. Ertl, *Europhys. Lett.* **75**, 868 (2006).
- [16] C. Qiao, H. Wang, and Q. Ouyang, *Phys. Rev. E* **79**, 016212 (2009).
- [17] J. Davidsen, M. Zhan, and R. Kapral, *Phys. Rev. Lett.* **101**, 208302 (2008).
- [18] M. Gameiro, K. Mischaikow and W. Kalies, *Phys. Rev. E* **70**, 035203(R) (2004).
- [19] N. T. Ouellette and J. P. Gollub, *Phys. Rev. Lett.* **99**, 194502 (2007); *ibid*, *Phys. Fluids*, **20**, 064104 (2008).
- [20] J. E. Pearson, *Science* **261**, 189 (1993).
- [21] H. Wang and Q. Ouyang, *Phys. Rev. Lett.* **99**, 214102 (2007).
- [22] S. Chakravarti, M. Marek, and W. H. Ray, *Phys. Rev. E* **52**, 2407 (1995).
- [23] I. Aranson, L. Kramer, *Rev. Mod. Phys.* **74**, 99 (2002).
- [24] B. I. Shraimana, A. Pumir, W. van Saarloos, P. C. Hohenberg, H. Chate, M. Hohen, *Physica D* **57**, 241 (1992).
- [25] H Chate, *Nonlinearity* **7**, 185 (1994).
- [26] S. Habib, G. Lythe, *Phys. Rev. Lett.* **84**, 1070 (2000); G. Lythe, *Physica D* **222**, 159 (2006).
- [27] J. H. Merkin, V. Petrov, S. K. Scott, K. Showalter, *Phys. Rev. Lett.* **76**, 3 (1996).